THE JOURNAL OF PHYSICAL CHEMISTRY B

ARTICLE

pubs.acs.org/JPCB

Molecular Dynamics Simulation Study of the Effect of DMSO on Structural and Permeation Properties of DMPC Lipid Bilayers

Jieqiong Lin, Brian Novak, and Dorel Moldovan*

Department of Mechanical Engineering, Louisiana State University, Baton Rouge, Louisiana 70803, United States

ABSTRACT: We present molecular dynamics simulations of dimyristoylphosphatidylcholine (DMPC) lipid bilayers in the presence of dimethyl sulfoxide (DMSO). The MD simulations focus on understanding the effect of 3 mol % DMSO on structural and permeation properties of DMPC bilayers. The potential of mean force (PMF) and the diffusivity profiles along the normal direction to the bilayer were calculated for water and DMSO molecules in systems containing 0 and 3 mol % DMSO. The simulation results indicate that while the presence of DMSO has only a small effect on diffusion coefficients of both water and DMSO molecules, it affects significantly the corresponding transmembrane free energy profiles. Using the free energy profiles and diffusivities for water and DMSO and by employing an inhomogeneous solubility-diffusion model we calculated the permeability coefficients. Our simulations show that the increase of the concentration of DMSO in the solution to 3 mol % leads to a significant increase, by about 3 times, of the permeability of water through a DMPC bilayer; a permeability increase that might explain in part the unusual ability of DMSO, even at relatively low concentrations, to reduce the osmotic pressure imbalance present during cryopreservation protocols.

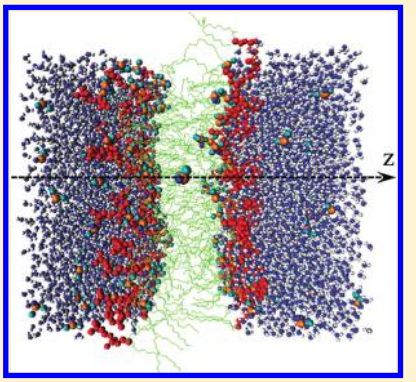

INTRODUCTION

Lipid bilayers are the basic structures that are used by living organisms to form their cell membranes which separate the cell interior from the surrounding environment and act as barriers between the inside and outside of a cell. Understanding the transport mechanism of various molecules across membranes is of great importance for many biological processes and a key ingredient in advancing the development of many technologies such as cryopreservation of biomaterials,[1,2] drug delivery,[3,4] and gene therapy.[5] Most small uncharged molecules, such as water, oxygen, and various drugs, are transported through membranes passively, via basal pathways, at appreciable rates whereas larger or charged molecules, such as ions, sugars, and amino acids, need active regulatory mechanisms assisted by specialized proteins.[6] Important cellular processes, such as rapid attainment of osmotic balance across plasma membranes in response to rapid changes of various physical and/or chemical variables, depend crucially on the existence of a basal pathway for water to move across membranes.

There are many solutes such as methanol, trehalose, glycerol, and DMSO that have the ability to modulate basal permeation properties of cell membranes. This modulation is very important in many cell biology and medical applications. In addition, these chemicals have long been utilized to minimize freezing injury during freezing preservation. The characteristic structural changes in membranes induced by them are presumed to play a major part in the outcome of cryopreservation in cell biology. Of all these chemicals, DMSO is of particular interest. DMSO is a small amphiphilic molecule consisting of a hydrophilic sulfoxide group (S═O) and two hydrophobic methyl groups. In addition to being a very good membrane permeability enhancer, DMSO also has the ability to induce cell fusion and cell differentiation.[2] Several experimental studies, using X-ray diffraction,[7] differential scanning calorimetry,[8] NMR, neutron diffraction, and infrared spectroscopy,[9] have been performed to investigate the effect of DMSO on various structural and thermodynamic properties of phospholipid bilayers. Despite the extensive experimental efforts, the understanding of the molecular basis for the effect of DMSO on lipid membranes is far from complete.

Molecular simulations provide important mechanistic insights into the interaction of various small molecules with lipid bilayers.[10,11] Recently, several hundred nanosecond-long *all-atom*[12−16] and *coarse-grained*[17] molecular dynamics (MD) simulations have been performed to investigate the effect of DMSO on various phospholipid bilayers. Sum and de Pablo performed MD simulations of lipid bilayers in the presence of various DMSO concentrations.[16] Their study showed that DMSO molecules penetrate deep into the lipid bilayer and accumulate mainly in a region below the lipid head groups and act as spacers that enhance lipid−lipid separation leading to a significant increase in the area per lipid. Their simulation results also indicate that the bilayer structural changes are mainly due to the DMSO induced dehydration close to the bilayer solvent interface and to the direct interaction of DMSO with the inner bilayer region. These modes of interaction with bilayers are generic for a larger class of small amphiphilic molecules, including short chain alcohols.[18,19]

Received: August 23, 2011
Revised: December 20, 2011
Published: December 22, 2011

Another recent MD simulation study by Notman et al.,[17] employing a *coarse-grained* model, found that, at higher concentration, DMSO has the ability to induce water pores in lipid bilayers, which could be a possible mechanism for the enhancement of membrane permeability to hydrophilic and charged molecules. These findings were confirmed later by Gurtovenko et al.[12] in an *all-atom* MD simulation study of dipalmitoylphosphatidylcholine (DPPC) lipid bilayers study in which they also demonstrated that, depending on its concentration, DMSO exhibits three distinct modes of action. At low concentrations (<7.5 mol %), DMSO induces an increase in the area per lipid. This increase is also associated with a corresponding thinning of the membrane. At larger concentrations (10−20 mol %), DMSO induces formation of water pores in the membrane. DMSO may even lead to disintegration of the bilayer structure when DMSO concentration exceeds 20 mol %. The MD simulation study of DMPC bilayers in the presence of 11.3 mol % DMSO of Moldovan et al.[14] provides additional insight into the mechanism of pore formation in lipid bilayers. Specifically, Moldovan et al. rationalize the pore nucleation process in terms of a simplified free energy model that includes the entropy of pore shape and the DMSO-induced lowering of both lipid bilayer line tension and the corresponding barrier for pore creation. Diffusion of DMSO through lipid bilayers in the presence of a concentration gradient was investigated by Leekumjorn and Sum using MD with a double-lipid-bilayer system geometry.[13] Given the inherent MD time-scale limitations they used the simulation results to estimate the required parameters that were then applied to Fick's diffusion laws and modeled DMSO concentration profile in the system as a function of time.

In this work, we study the effect of DMSO on the properties of DMPC bilayers, in the absence of transient pores, and evaluate the permeability coefficients for both water and DMSO molecules at low DMSO concentration. Given that the permeation of both water and DMSO through lipid bilayers is too slow to occur during typical MD simulation time scale, we evaluate the permeability coefficients indirectly by employing an inhomogeneous solubility-diffusion model and by computation of the free energies and diffusion coefficients profiles across the DMPC bilayer. The ultimate goal is to obtain a better understanding of the molecular mechanism and the parameters that determine the enhancement by DMSO of basal bilayer permeability in the absence of pores.

METHODS

Simulation Details. MD simulations were performed on two DMPC bilayer systems in which the concentration of DMSO was 0 mol % (pure water) or 3 mol % with periodic boundary conditions in all directions. Throughout the entire paper when referring to the concentration of the water−DMSO solution we used the mole percent (mol %); the quantity that is equal to the mole fraction multiplied by 100. In our case, mol % is given by the number of DMSO molecules divided by the sum of the number of DMSO and water molecules and then multiplied by 100. Both systems contain 96 lipid molecules (48 lipids in each leaflet) and 5422 water molecules (the 3 mol % system contains an additional 162 DMSO molecules). The initial configuration of the DMPC−DMSO bilayer system was generated from the pure water system by randomly replacing 162 water molecules with DMSO molecules. Additional information regarding the preparation and initial equilibration of the DMPC bilayer−pure water system can be found in our previous studies.[14,19]

All the simulations were performed with the GROMACS 4.0 simulation package.[20] The force field parameters for lipids for both bonded and nonbonded interactions were taken from Berger et al.[21] while the partial charges were taken from Chiu et al.[22] The force field parameters of Bordat et al.[23] were used for DMSO and the simple point charge (SPC) model for water.[24] All simulations were performed at constant pressure of 1.0 bar using a Berendsen barostat and semi-isotropic coupling with time constants of 5.0 ps in the directions parallel to the bilayer surface and 4.0 ps in the direction normal to the bilayer surface. The temperature was held constant at 323 K, which is above the phase transition temperature of DMPC bilayers in both pure water and 3 mol % DMSO systems (recall that it has been observed experimentally that DMSO has the ability to increase the phase transition temperature of DMPC bilayers from gel phase to liquid-crystalline phase[9]). At T = 323 K, both systems studied were in the liquid-crystalline phase. All non-water bond lengths were constrained by using the LINCS[25] algorithm. Water bonds and angles were constrained using the SETTLE algorithm.[26] For short-range nonbonded interactions, GROMACS uses a twin range cutoff. The inner cutoff was 0.98 nm. Forces due to van der Waals interactions in the range from 0.98 to 1.4 nm were evaluated every 10 steps. The long-range electrostatic interactions were treated using the particle mesh Ewald (PME) algorithm,[27,28] with a 0.1176 nm grid spacing, of order 4, and tolerance of 10^{-5}. We used an integration time step of 2.0 fs. The energy minimization procedure, based on the steepest descent algorithm, was applied to the initial structures prior to the actual MD runs. The bilayers in both 0 and 3 mol % DMSO systems were prepared initially by 50 ns MD runs, out of which the last 25 ns were used for evaluation of various averaged properties.

The main goal of this study was to investigate the effect of 3 mol % DMSO solution compared to pure water on the permeability of water and DMSO molecules in DMPC bilayers (cryopreservation experiments often employ a concentration of 2.5 mol %[2]). Evaluation of the permeability coefficients required calculation of the profiles along the perpendicular direction to the bilayer of both free energies (the so-called potentials of mean force (PMFs)) and diffusivities of water and DMSO molecules. Mass densities, charge densities, electrostatic potentials, and the orientations of water and DMSO dipole moments were calculated as a function of distance from the bilayer center, the angular and the corresponding residence time distributions of the DMPC P−N vector orientations were calculated, and the number of hydrogen bonds per water molecule was calculated for water molecules in the ester group and tail regions of the bilayers.

PMF and Diffusion Coefficient Calculation. The constraint force method[29,30] was used to calculate the PMFs and diffusivities as a function of the distance from the center of the bilayer to the center of mass of a water or DMSO molecule in the direction normal to the bilayer (z-axis). A total of 31 distances (0.0, 0.107, 0.224, 0.341, ... 3.5 nm) were chosen distributed between the bilayer center, located at z = 0 nm, and a reference point located in solution at z = 3.5 nm, far from the lipid-solvent interface. To obtain starting configurations the constrained water or DMSO molecule was dragged from one distance to an adjacent one by changing the constraint distance and performing an energy minimization. Figure 1a depicts the cross-sectional view of the DMPC bilayer in 3 mol % DMSO−water solution in which the distance from the bilayer center along the z-axis of the

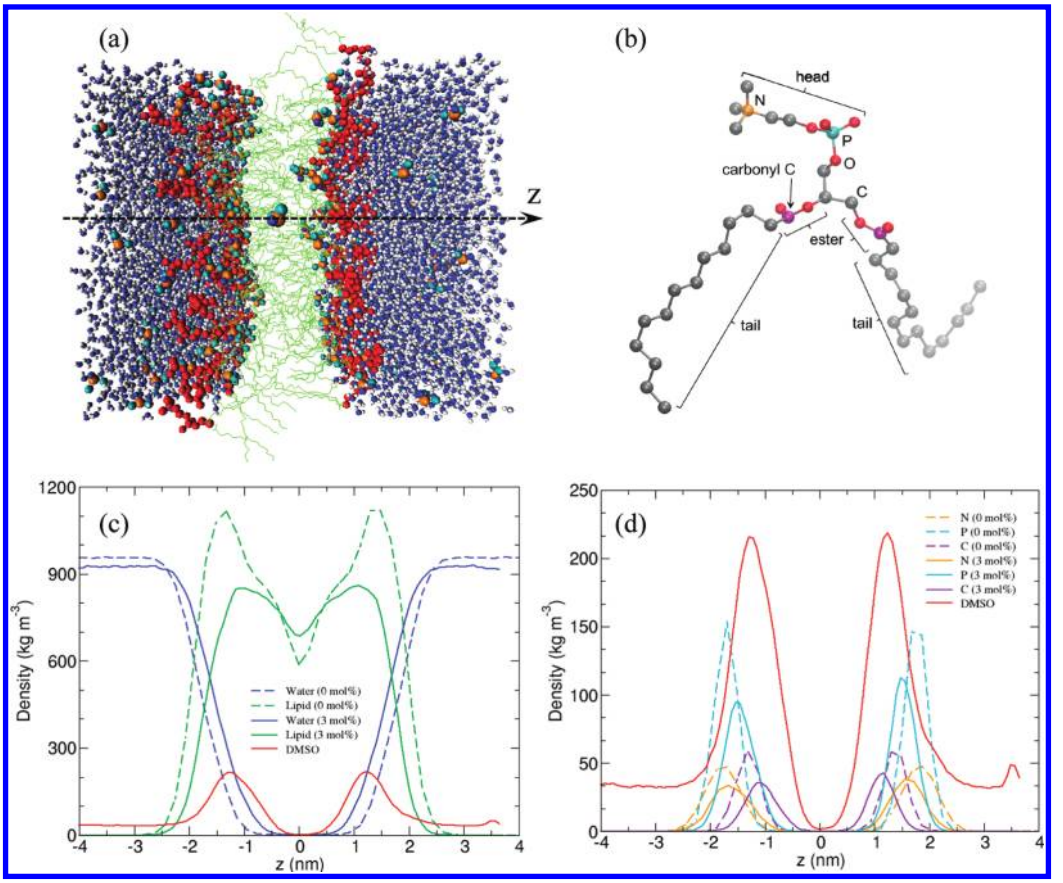

Figure 1. (a) Cross sectional view of the DMPC membrane in the 3 mol % DMSO solution. Red spheres are used to represent the DMPC head groups (hydrophilic) and green lines refer to DMPC tail groups (hydrophobic). In DMSO, the spheres are shown as orange for sulfur atoms, blue for oxygen atoms, and green for methyl groups. The constrained DMSO molecule located at the center of the bilayer is drawn in a bigger size compared to other DMSO molecules. (b) Molecular structure of DMPC. (c) Mass density of lipids, water, and DMSO along the bilayer normal in both 0 mol % and 3 mol % DMSO systems. (d) Mass densities of specific atoms such as phosphorus, nitrogen, and carbonyl carbon atoms of the ester groups along the bilayer normal in both the 0 mol % and 3 mol % DMSO systems. $z = 0$ corresponds to the center of the bilayer.

large-drawn DMSO molecule is constrained using the SHAKE[31] algorithm. The average constraint force was determined for each distance and these average forces were numerically integrated to calculate the potential of mean force.[11] The diffusivity profile as a function of distance along the z-axis was calculated by time integrating the local time autocorrelation functions of the fluctuations of the constraint forces.[11] In most cases 4 ns of simulation time was used for equilibration at each distance followed by 8 ns of production time. The exception was for the 3 mol % DMSO system when the water molecule was constrained at distances between 0.0 and 2.447 nm. For those distances, 32 ns were used for equilibration followed by 12 ns of production time. The production time was used for calculations of the average constraint forces and the autocorrelation function of the fluctuations of the constraint forces. The permeability coefficients for water and DMSO molecules were calculated using the inhomogeneous solubility-diffusion model and are related to an integral over distance across the bilayer involving the PMF and local diffusivities obtained using the constrained molecule method.[11]

RESULTS AND DISCUSSION

Mass Density Profiles Across DMPC Bilayers. Valuable information about the structural changes of the DMPC bilayer can be obtained by analyzing the mass distribution of various molecules or molecular groups along the direction perpendicular to the bilayer. Parts b and c of Figure 1 depict the structure of a DMPC molecule and the mass density profiles of lipids, water, and DMSO molecules along the normal direction to the bilayer in both 0 mol % and 3 mol % DMSO solutions. For the lipids, the mass density profile indicates the distribution of the atoms comprising the lipids along the normal direction to the bilayer. These profiles are determined by dividing the simulation box along the normal direction to the bilayer into a number of thin slices of equal thickness and by finding the mass density of the atoms located in each slice followed by time averaging over a large number of snapshots evenly distributed over the production simulation time interval (i.e., the last 25 ns of the 50 ns simulation). The density profiles have been shifted for clarity such that for both systems the center of the bilayers are located at $z = 0$. On the basis of the lipid and water density profiles one can identify three distinct regions of the bilayer-solvent systems: (i) the bulk aqueous phase, (ii) the lipid-solvent interface region containing of lipid head groups, water, and DMSO, and (iii) the interior of the bilayer where the tails of the two leaflets meet. The water density is high in the aqueous region, decreases steadily in the lipid-solvent interface region, and reaches very low values in the middle of the bilayer where the hydrophobic lipids acyl chains

dx.doi.org/10.1021/jp208145b |J. Phys. Chem. B 2012, 116, 1299–1308

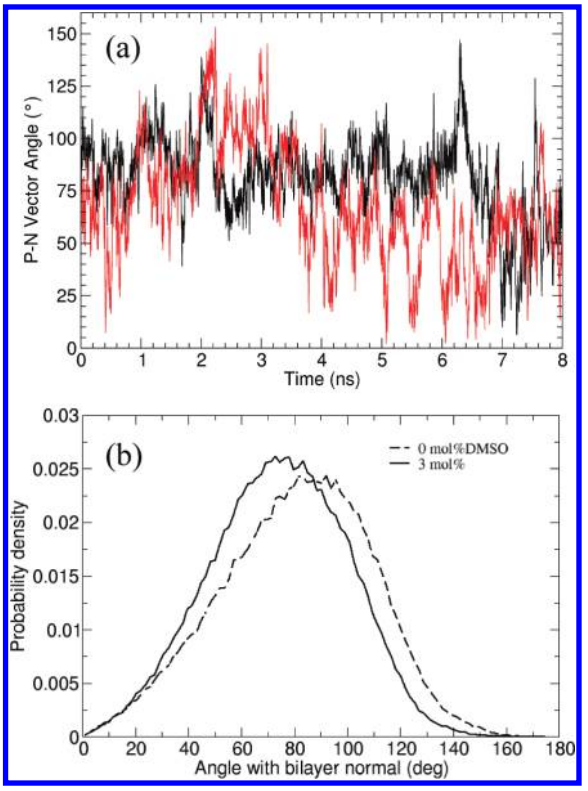

Figure 2. (a) Time evolution of the angle between the P−N vector of the DMPC headgroup and the bilayer normal for two arbitrarily chosen lipids in the 3 mol % DMSO system. (b) Time-averaged distribution of the angle between the P−N vectors of the DMPC head-groups and the outwardly directed bilayer normal in both pure water and 3 mol % DMSO solutions.

reside. There is a pronounced peak on the DMSO mass profile indicating that DMSO penetrates deep and accumulates into the lipid/water interface region and occupy positions beneath the lipid head groups in the vicinity of the ester groups. The location of the peak is determined by the amphiphilic character of DMSO in which the two methyl groups interact favorably with the hydrocarbon acyl chains while the highly polar sulfoxide group can interact favorably with lipid heads. The DMSO mass density peak is located in the same region as the mass density peaks of the atoms delimiting the polar portion of the lipids (phosphorus and nitrogen) and the connection with the hydrophobic tails (carbonyl carbon atoms of the ester groups) as indicated in Figure 1d. It is important to notice that, in the relatively small simulation system (e.g., 96 lipids, 5422 waters, and 162 DMSO molecules), the accumulation of DMSO inside the lipid bilayer leads to an effective decrease of the concentration of DMSO in the bulk solution (far from the bilayer−solvent interface) from the initial 3 mol % value to about 0.9 mol %.

Orientation of Lipid Head-Groups (P−N Vectors). The effect of DMSO on the orientation of the lipid head-groups was studied by evaluating the orientation distribution of the angle between the P−N vector, connecting the phosphate phosphorus atom to the choline nitrogen atom, and the outwardly directed bilayer normal. Figure 2a depicts the time evolution of the headgroup orientation for two randomly chosen lipids in the 3 mol % DMSO system. This shows that the orientation of individual head-groups may change frequently in the 0° to 150° interval and, in just a few nanoseconds, may assume multiple times very small or very large values. Consequently, the corresponding headgroup orientation distribution functions are expected to be fairly wide. Figure 2b shows that, indeed, the lipid head-groups orientation distributions functions are fairly wide in both pure water and 3 mol % DMSO systems and reach their maximum values near 88° and 75° for the pure water and the 3 mol % DMSO systems, respectively. These orientation angles at which the distributions reach their maximum values indicate that, in both simulated systems, the DMPC head-groups prefer orientations that are nearly parallel to the bilayer surface.

The overall tendency of the lipid headgroup dipoles to adopt a more parallel orientation to the bilayer is favored by the lowering of the free energy component due to electrostatic dipole−dipole interaction associated with these bilayer configurations. As each lipid headgroup can be modeled as an in plane point dipole (the plane of the bilayer leaflet) surrounded by a screening asymmetric dielectric medium (i.e., the solvent of a dielectric constant of about 78 on one side of the leaflet and the hydrophobic lipid tails region of the bilayer interior of a dielectric constant of about 1), every one of these dipoles interacts with the field from all the other dipoles contributing to the overall electrostatic interaction free energy component. Given that, in average, the dipoles are tilted with respect to bilayer normal, they may be split into two components one parallel and one perpendicular to the bilayer. The perpendicular parts become static dipoles and their interactions will be repulsive and scale with distance as r^{-3} term that is less favorable energetically.[32] On the other hand, since the in-plane components are allowed to rotate freely around the membrane normal,[32] their fluctuations will lead to attractive interactions that scale as r^{-6}. The intricate combination of these electrostatic interaction terms together with those due to the nearby dipolar moments of the polarized water and DMSO molecules will play an important role in establishing the average orientation angle of lipid head-groups. Specifically, the interaction between DMSO dipolar moment and the DMPC head-groups dipoles may explain, in part, the shift in the P−N vector angle distribution in the presence of DMSO. That is, the polar DMSO molecules, located mostly below the head-groups (see Figure 1d), will tend to rotate the P−N vectors in the 3% system to point more outwardly so they can line-up more closely with the DMSO dipole moment vectors, thus minimizing the dipole−dipole electrostatic interaction.

The presence of DMSO increases the area per lipid which is expected to increase the conformational mobility of the lipids. This can be characterized by the residence time distributions of the lipid head group P−N vector angles with the bilayer normal vector. The residence time distribution was calculated by considering the lipids with P−N vector angles near the maximum in the angle distribution (shown in Figure 2b) at a time after equilibration. The number of these lipids divided by the total number gave a concentration, $C(0)$. If at any subsequent time, the P−N vector angle of a lipid passed outside of some range of its initial angle, then it was no longer counted in the concentration, $C(t)$, for all remaining time. All time origins in which the concentration fell to zero within the span of the simulation data were considered, and averaged. The residence time distribution is the concentration divided by the integral of the concentration over time:

$$E(t) = \frac{C(t)}{\int_0^\infty C(t)\,\mathrm{d}t} \qquad (1)$$

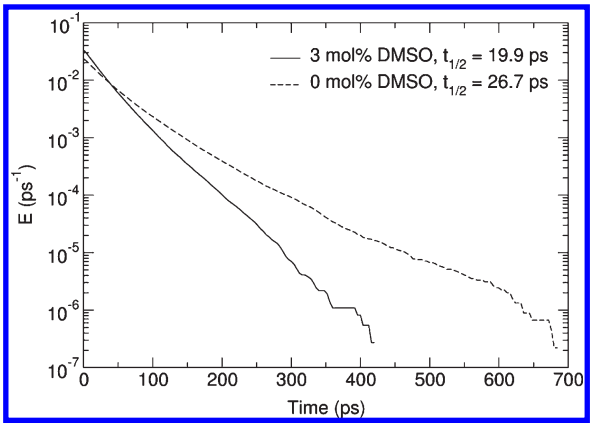

Figure 3. Residence time distributions (E) for P−N vector angles starting within 25° of the maxima in the angle distributions in Figure 2b and residing within ±15° of their initial angles. The times for E to decay to half of its initial value are shown in the legend. The distribution for the 3 mol % case decays faster, indicating an increased conformational mobility of the lipids.

A plot of residence time distributions vs time for the 0 mol % and 3 mol % systems is depicted in Figure 3, which shows that the time scale for changing the P−N vector orientation is indeed shorter in the 3 mol % system.

Charge Density and Electrostatic Potential. The average presence of an electric dipole component along the normal direction in the bilayer-solvent interfacial region gives rise to an electrostatic potential across a leaflet of the membrane. Moreover, since the presence of DMSO has a significant effect on the P−N vector angle distribution, it is expected that this will also affect the charge density and electrostatic potential across the bilayer. This is because the polar head groups have relatively large partial charges on their atoms.

Figure 4 shows the average charge densities across the bilayer obtained from the simulations of the 0 mol % and 3 mol % DMSO systems. Figure 4a, shows the total charge density as well as the contributions from the lipids and water in the 0 mol % DMSO system. The charge distribution due to lipid head groups is mirrored and almost compensated by the opposite charge due to the water dipoles of the polarized water molecules located in the bilayer−solvent interface region. In fact, as shown in Figure 4a, the comparison of the water and the total charge distributions indicate that the water molecules in the interfacial region overcompensate the lipid charge distribution. The same trend is observed is the 3 mol % DMSO system although in the presence of DMSO, as shown in Figure 4b, both the lipid and water charge density profiles are not as smooth as in the pure water system. This can be attributed to in plane disordering effect due to the increased spacing between the lipids heads and the presence of a larger number of water and DMSO molecules in the interfacial region of the bilayer.

The electrostatic potential, $\psi(z)$, across the lipid bilayer can be calculated from the Poisson equation by double integrating the charge density $\rho(z)$:

$$\psi(z) - \psi(z_0) = -\int_{z_0}^{z} dz' \int_{z_0}^{z'} \rho(z'')\, dz'' \qquad (2)$$

where $\psi(z_0)$ represents the electrostatic potential inside the solvent region at z_0 far away from the bilayer surface. In our calculations, we assume $\psi(z_0) = 0$ at the distance furthest from

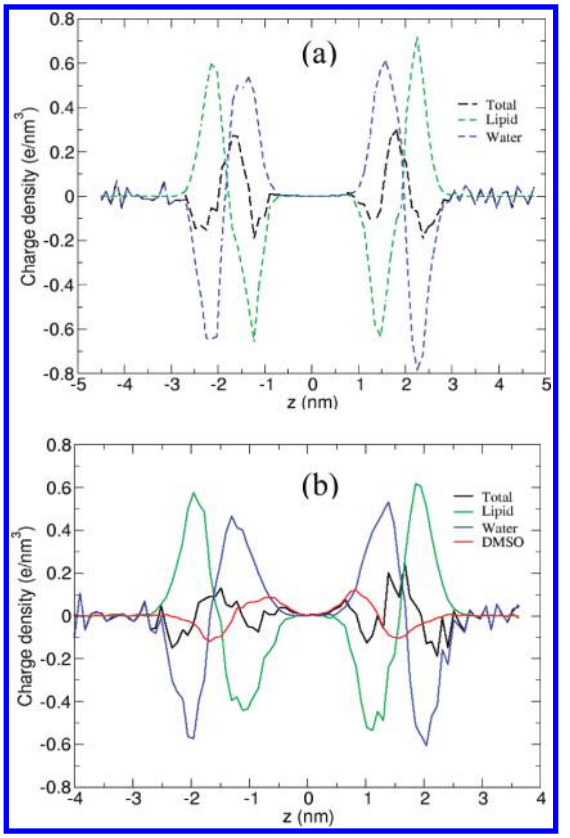

Figure 4. Local charge density contributions from lipids, water and DMSO molecules in (a) 0 mol % DMSO system and (b) 3 mol % DMSO systems. z = 0 corresponds to the center of the bilayer.

the bilayer center. Figure 5a shows the profiles of the total electrostatic potentials across the lipid bilayer in both 0 mol % and 3 mol % DMSO systems. In both systems the interior of the bilayer has a positive potential relative to the aqueous surrounding. The actual potential drop between the bilayer interior and the solvent (trans-leaflet potential) is about 575 mV and 775 mV in the 0 mol % and 3 mol % DMSO respectively. Interestingly the presence of DMSO leads to an increase of the trans-leaflet potential by about 35% relative to the pure systems. These values are in very good agreement with other simulation[33] and experimental results.[34] Using the unique MD simulations capability one can gain additional insight into the origin of the trans-leaflet potential by splitting the total potential into the corresponding terms caused by different types of molecules. Figure 5b shows the contributing terms to the total electrostatic potentials due to the lipids, water, and DMSO molecules in both simulated systems. As with the charge distribution, the electrostatic potential due to water molecules mirrors and slightly overcompensates the potential component due to lipid heads. As expected, the potential component due to the DMSO molecules, although of smaller magnitude, has the same sign and shape as the component due to the water molecules. Moreover, as indicated in Figure 5(b) the presence of DMSO leads to an increase of the potential component due to the lipid heads. This increase can be attributed to the slight change of the average orientation of the P−N vectors toward a more out-of-plane orientation (see Figure 2b). As mentioned previously, this change in orientation of the P−N vector leads to an average increase of the normal component of the lipid dipolar moments which in turn leads to a slightly larger

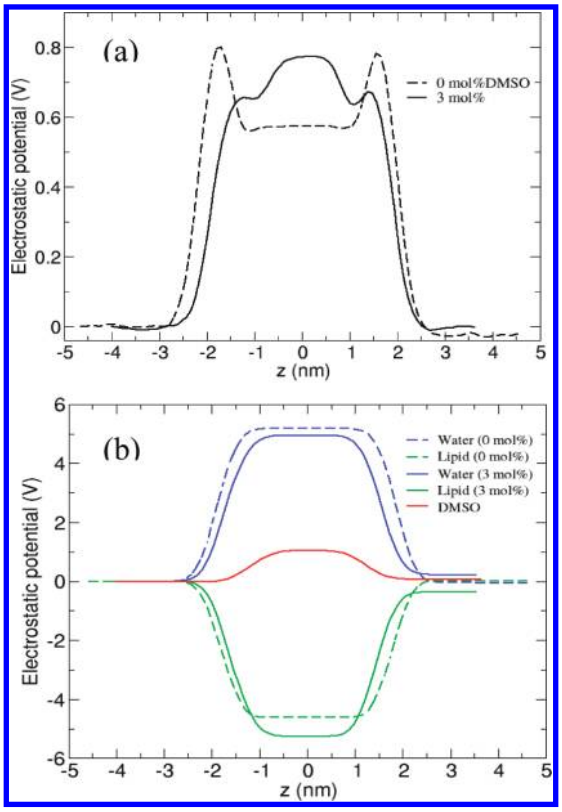

Figure 5. (a) Total electrostatic potential across the bilayer in both 0 mol % (dashed line) and 3 mol % DMSO (solid line) systems. (b) Contributions of water, lipids, and DMSO to the total electrostatic potential in both 0 mol % (dashed lines) and 3 mol % DMSO (solid line) systems.

lipid dipolar charge and larger potential change across the bilayer-solvent interface.

DMSO and Water Electric Dipole Orientation Across Lipid Bilayers. Additional information about the DMSO and water ordering in the vicinity of the bilayer−solvent interface (hydration layer) can be obtained from studying the time averaged projections of DMSO and water electric dipole unit vectors $\vec{\mu}$ onto the bilayer normal unit vector $\vec{n}$, which can be written as

$$\langle \cos\theta(z) \rangle = \langle \vec{\mu}(z) \cdot \vec{n} \rangle \quad (3)$$

where θ is the angle between the electric dipoles and normal vector to the bilayer; z is the z-component of the center of mass of the DMSO or water molecule. The mean cosine value profile is obtained by averaging, when the system is in the equilibrium regime, over dipolar orientations of all DMSO or water molecules present in the corresponding bins and over a large number of equilibrium states. Figure 6 shows the profiles of the averaged electric dipole projections in 0 mol % and 3 mol % systems for water and DMSO (only in 3 mol % system) molecules. Notice that a zero mean cosine average far from the bilayer center corresponds to a random orientation of the electric dipoles and that the normal unit vector, $\vec{n}$ points along the positive z direction on both sides of the bilayer. Consequently, by symmetry, the cosine average has the opposite sign in the two regions. As revealed by Figure 6, in or near the bilayer, both the water and DMSO molecules prefer to orient themselves such

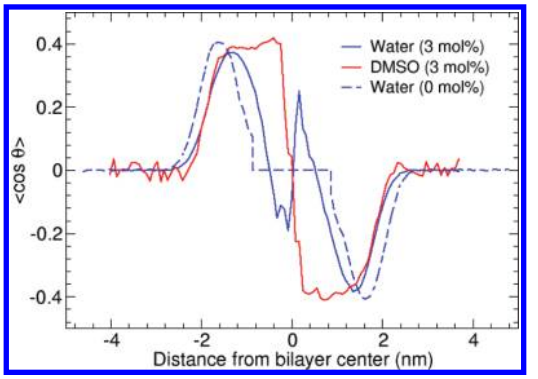

Figure 6. Average of the cosine of the angle between dipole moment vectors of DMSO and water molecules and the outward normal to the upper leaflet (positive distance) as a function of the distance from the bilayer center in both 0 mol % and 3 mol % DMSO systems.

that their electric dipolar moments are oriented away from the outward bilayer normal. In fact, the maximum magnitude of $\langle \cos\theta \rangle$ corresponds to an angle that is about 180° different from the average P−N vector orientation. The P−N vector is a good approximation to the dipole moment vector of a DMPC molecule. The dipoles of the DMSO and water molecules in the bilayer point in the opposite direction of DMPC dipoles since this is the most energetically favorable orientation. For water, the ordering peak is located slightly more outward, along the bilayer normal direction, compared to the peak corresponding to the lipids (see Figures 1c and 6). The electric dipole ordering peaks for DMSO are wider and extend deeper into the bilayer than the corresponding peaks for water. The DMSO dipoles maintain their alignment in the opposite direction of the DMPC dipoles almost up to the bilayer center. Since only a few water and DMSO molecules penetrate deep into the lipids acyl chains region, the statistics of averaging is poor in that region resulting in noisy orientation profile curves for both molecular species. Comparing the water orientation profiles in 0 mol % and 3 mol % DMSO solutions indicate that DMSO leads to a decrease in the separation distance between the centers of the two hydration layers present on both sides of the membrane which is directly correlated to the decrease of the bilayer thickness in the presence of DMSO.

Number of Hydrogen Bonds per Water Molecule Inside the Bilayer. The number of hydrogen bonds per water molecule was calculated in the regions of the bilayer containing the ester group oxygen atoms and in the bilayer tail region. A hydrogen bond was defined to exist when the donor−acceptor distance was less than or equal to 0.35 nm and the donor-hydrogen-acceptor angle was less than 30° from linear alignment. In this system, the only donor is the water oxygen atom. The acceptors considered are the water oxygen, the DMSO oxygen, and the four ester oxygen atoms. The two ester group regions were defined by averaging the upper and lower boundary positions (z direction) of the ester group oxygen atoms over all frames. The tail region was defined as the region between the two ester group regions, except that no water molecules within the donor−acceptor cut off distance from an ester group oxygen atom were counted in this region.

Table 1 shows the number of hydrogen bonds per water molecule between water molecules and ester group oxygen atoms, DMSO molecules, and other water molecules; and the number density of water in the ester group and tail regions of the bilayer. One might

Table 1. Number of Hydrogen Bonds per Water Molecule and Water Number Density in the Regions Containing the Ester Group Oxygen Atoms and in the Tail Region

	Ester Group Region					
	number of water hydrogen bonds per water molecule					
system	ester	DMSO	non-water	water	total	ρ_{water} (nm^{-3})[a]
0 mol %	0.42 ± 0.02	--	0.42 ± 0.02	0.64 ± 0.02	1.062 ± 0.007	6.3 ± 0.3
3 mol %	0.26 ± 0.01	0.123 ± 0.004	0.38 ± 0.01	0.74 ± 0.01	1.122 ± 0.005	6.7 ± 0.2
	Tail Region					
	number of water hydrogen bonds per water molecule					
system	ester	DMSO	non-water	water	total	ρ_{water} (nm^{-3})
3 mol %	--	0.13 ± 0.03	0.13 ± 0.03	0.03 ± 0.01	0.16 ± 0.04	0.022 ± 0.004

[a] For comparison, the water density in bulk solvent is 32.0 and 31.0 nm^{-3} in the 0 mol % and 3 mol % cases, respectively. Uncertainties are two times the standard deviation of the mean.

expect that the addition of DMSO might increase the number of water hydrogen bonds with nonwater molecules (ester group oxygens + DMSO). However, in the ester group region, adding DMSO reduces the number of ester group hydrogen bonds and the number of nonwater hydrogen bonds actually decreases slightly with the addition of DMSO. Adding DMSO does allow more water molecules into the bilayer (increased density). With more water present, the number of water−water hydrogen bonds increases such that the total number of water hydrogen bonds also increases slightly. In the tail region, the number of water-DMSO hydrogen bonds is nearly the same as in the ester group region while the number of water−water hydrogen bonds is less than a quarter of this. This indicates that a DMSO molecule can carry a water molecule into the tail region, but clusters containing multiple water molecules are much less likely.

Free Energy Profiles. The PMF for water and DMSO molecules in both 0 mol % and 3 mol % DMSO systems were calculated as a function of the distance from the bilayer center by numerical integration of the average constraint forces acting on the constrained molecule at different positions. Parts a and b of Figure 7 show the PMFs calculated for water and DMSO molecules respectively in both systems. As shown in Figure 7a, the PMF profile for a water molecule located far from the bilayer center is flat in both systems. As the molecule approaches the bilayer center, the PMF increases steeply. In the pure water system, as the water molecule moves closer to the bilayer center, the PMF exhibits an obvious peak of about 27 kJ/mol, located near the center of the bilayer, followed by a slight decrease. In contrast, in the system containing DMSO, the PMF for the water molecules increases steadily, without a clear peak, until the center of the bilayer where it reaches a maximum value of approximately 23 kJ/mol. The peak near bilayer center and minima of the PMF at the bilayer center in the pure water system are due to the low lipid density at the bilayer center (see Figure 1c). In the system containing DMSO, this density minimum is not as pronounced, so there is no peak in the PMF other than that corresponding to the center of the bilayer. As documented in Figure 7a, the presence of 3 mol % DMSO into the DMPC bilayer system leads to a reduction of the free energy barrier for a water molecule by about 4 kJ/mol. As shown in the following sections the decrease of the barrier in the PMF profile affects significantly the water permeability coefficient in DMPC bilayers.

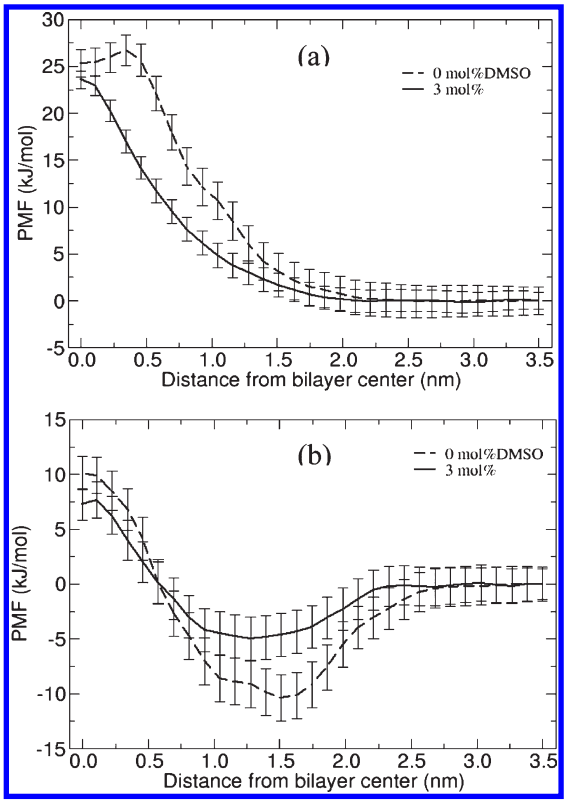

Figure 7. PMF profiles for (a) water molecules and (b) DMSO molecules along the normal direction to the DMPC bilayer in both 0 mol % and 3 mol % DMSO systems. Error bars are 2 times the standard deviation of the mean.

As illustrated in Figure 7b, the PMF profiles for a DMSO molecule moving across a DMPC lipid bilayer in both pure water system and the system containing DMSO look significantly different from the PMFs for the water molecule (see Figure 7a). Specifically, in both systems the PMFs for the DMSO molecule decrease continuously and reach a minimum value as the molecule moves from solvent into the DMPC bilayer. The minima are located approximately midway between the peaks corresponding to the lipid heads phosphate and the carbonyl group (see Figures 1d and 7b). Moreover, the profiles of the

dx.doi.org/10.1021/jp208145b |J. Phys. Chem. B 2012, 116, 1299–1308

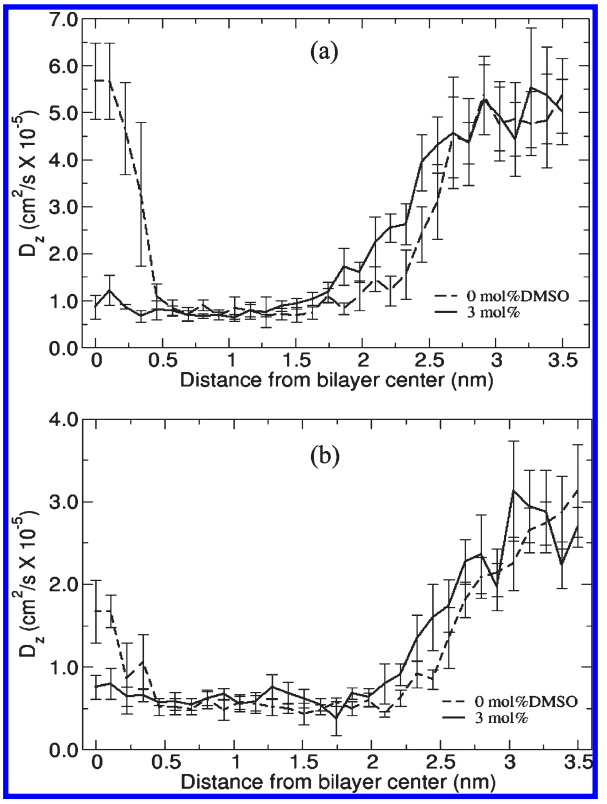

Figure 8. Profiles of the diffusion coefficient, $D(z)$, for (a) water molecules and (b) DMSO molecules along the normal direction to the DMPC bilayer in both 0 mol % and 3 mol % DMSO systems. Error bars are 2 times the standard deviation of the mean.

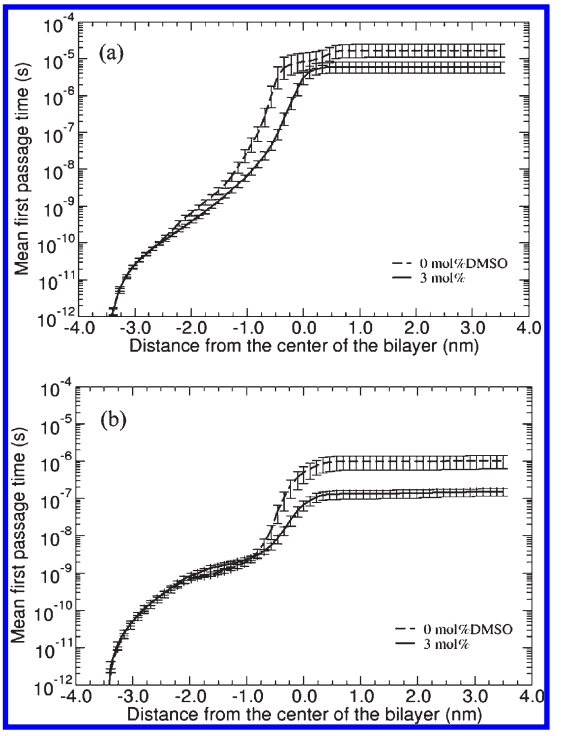

Figure 9. Mean first passage time for (a) a water molecule, and (b) a DMSO molecule starting from $z_0 = -3.5$ nm away from the bilayer center to move to a new location z along the bilayer normal in both 0 mol % and 3 mol % DMSO systems. Uncertainties (95.4% confidence interval) were determined by sampling from the distributions for the PMF and diffusivity for each point and calculating many mean first passage times.

PMFs around their minimum values are fairly flat over a relatively large interval comprising the distances from bilayer center located between 1.0 nm and about 1.75 nm. Unlike the pure water system, the PMF for the DMSO molecule in the 3 mol % DMSO system shows a much smaller decrease moving into the bilayer. Both PMF profiles show a fairly steep increase when the DMSO molecule moves toward the center of the bilayer where the PMFs reach their maximum values of approximately 10 and 7.5 kJ/mol in the pure water system and 3 mol % DMSO system, respectively. In both simulated systems the DMSO molecule experiences significantly lower PMF barriers compared to the water molecule. One can rationalize these characteristics in terms of differences in polarity of the two molecules. While water molecules are highly polar, the DMSO molecules with their slight amphiphilic character can be accommodated more easily into the hydrophobic interior of the bilayer.

Diffusion Coefficients. The diffusion coefficient profiles for water and DMSO molecules in both the pure water system and the system containing 3 mol % DMSO are plotted in Figure 8 as a function of the distance from the center of the bilayer. There are obvious similarities between the diffusion profiles for the two molecules in both systems indicating very similar diffusion mechanisms throughout the entire diffusion path spanning the bulk solution, the bilayer-solvent interface, and the interior of the bilayer. As shown in parts a and b of Figure 8, the water and DMSO diffusivities have the highest values in the solvent and decrease steeply and remain relatively constant as the molecules move through the bilayer-solvent interface toward the bilayer center. Interestingly, in the pure water system the diffusion coefficients for both water and DMSO increase rapidly upon moving toward the middle of the bilayer, an increase that is associated with the existence of a larger free volume in the region where the tails of the lipids comprising the two leaflets meet (see Figure 1c). One can also conclude that with the exception of a narrow region in the bilayer midsection the presence of DMSO seems to have a very limited effect on the diffusivity of both water and DMSO molecules.

Molecular Mean First Passage Times Through the Bilayers (MFPT). In the high friction limit of the diffusive motion, the mean first passage time for a molecule to reach a distance from the bilayer center z_2 when starting from a distance z_1 can be calculated by the following equation:[35,36]

$$\langle \tau_i \rangle = \int_{z_1}^{z_2} \frac{e^{PMF_i(x)/k_B T}}{D_i(x)} dx \int_{-3.5\ \mathrm{nm}}^{x} e^{-PMF_i(y)/k_b T}\, dy \qquad (4)$$

The mean first passage time curves are shown in Figure 9 for (a) water and (b) DMSO. The times required for a molecule located initially in the bulk solution on one side of the bilayer far from the bilayer-solvent interface (i.e., at $z_1 = -3.5$ nm) to cross to the bulk solution on the other side ($z_2 = 3.5$ nm) are shown in Table 2. This indicates that the mean first passage times for both water and DMSO molecules are in the microseconds range, far beyond the reach of direct MD simulation time scale. Interestingly, for both water and DMSO, the times are more than an order of magnitude smaller in the 3 mol % DMSO systems.

Permeability Coefficients. Using the free energy profiles and the diffusivities for water and DMSO and by employing an

Table 2. Permeabilities and Mean First Passage Times for Water and DMSO Molecules to Diffuse (across a DMPC Bilayer) between Two Points Located, Deep into the Solvent, at $z_1 = -3.5$ nm and $z_2 = 3.5$ nm on Either Side of the Bilayer in both 0.0 mol % and 3.0 mol % DMSO Systems[a]

molecule	DMSO [mol %]	P (cm/s)	$\langle\tau\rangle$ (μs), from −3.5 to 3.5 nm
water	0.0	0.0119 (0.0043, 0.0051)	16.2 (6.2, 8.6)
DMSO	0.0	4.1 (1.5, 1.9)	1.01 (0.39, 0.64)
water	3.0	0.037 (0.011, 0.013)	5.77 (1.6, 2.24)
DMSO	3.0	5.58 (1.98, 1.75)	0.15 (0.034, 0.045)

[a] The values in parentheses are error bars (−, +) for a 95.4% confidence interval.

inhomogeneous solubility-diffusion model one can calculate the permeability coefficients through the DMPC bilayer. The values of the permeability coefficients are related to the local properties and can calculated according to the following relation:[11]

$$P_i = \frac{1}{R_i^p} = \frac{J_i}{\Delta c} \tag{5}$$

where J_i is the flux of molecules of species i, Δc is the concentration difference, P_i is the permeability coefficient and R_i^p is the permeation resistance given by

$$R_i^p = \int_{z_1}^{z_2} \frac{e^{PMF(z)/k_B T}}{D(z)}\, dz \tag{6}$$

As shown in Table 2, in the pure water system (or the limiting case of infinitely diluted DMSO solution system when a single DMSO molecule is present in the solution), the permeability coefficients are 0.0119 and 4.1 cm/s for water and DMSO respectively. The value for water is within the range of experimentally measured values (e.g., 4.0×10^{-4} to 2.4×10^{-2} cm/s) for fluid-phase DMPC.[37] The permeability of both water and DMSO molecules increase in the presence of 3 mol % DMSO. While the DMSO molecules experience only a modest 36% increase of the permeation coefficient, the permeability of water molecules increases significantly, by approximately 300%, from 0.0119 to 0.037 cm/s. This significant increase of permeation coefficient for water is mainly a direct consequence of the decrease of the water free energy barrier (PMF) located at the center of the lipid bilayer, in the presence of 3 mol % DMSO (see Figure 7(a)).

CONCLUSIONS

Our MD simulation study has shown that at relatively low concentration, DMSO molecules penetrate and diffuse deep into DMPC bilayers and concentrate in the region located below the lipids polar head-groups. At 3 mol % DMSO concentration, the DMPC bilayer remains intact on a time scale of tens of nanoseconds (i.e., no stable or transient pores form in the bilayer), but the DMSO molecules have a strong effect on the area per lipid, the bilayer thickness, the orientation of the lipid heads with respect to the bilayer normal, and on trans-leaflet electrostatic potential. The calculation of the potential of mean force (PMF) and the diffusivity profiles along the direction normal to the bilayer for water and DMSO molecules indicate that while the presence of DMSO has only a small effect on diffusion coefficients of both water and DMSO, it affects significantly the corresponding trans-membrane free energy profiles. Using the free energy profiles and diffusivities for water and DMSO and by employing an inhomogeneous solubility−diffusion model, we calculated the corresponding permeability coefficients. The values of the permeability coefficients, related to an integral over the local free energy and diffusivities, enable a direct comparison between computational model and experiments. Our simulations show that in the pure water bilayer system the permeability coefficients are 0.0119 and 4.1 cm/s for water and DMSO respectively; values that are in good agreement with experimental results. Interestingly, the increase of the concentration of DMSO in the solution to 3 mol % leads to a significant increase, by about 300%, of the permeability of water through DMPC bilayer. This permeability increase might explain in part the unusual ability of DMSO, at relatively low concentrations, to reduce the osmotic pressure imbalance present during cryopreservation protocols.

AUTHOR INFORMATION

Corresponding Author

*Telephone: 225-578-6488. Fax: 225-578-5924. E-mail: dmoldo1@lsu.edu.

ACKNOWLEDGMENT

This work was supported in part by USDA Grant No. 2009-35603-05055 and by NSF-EPSCoR LA-SiGMA Grant No. EPS-1003897. Computer Resources were provided by LONI and HPC@LSU.

REFERENCES

(1) Arakawa, T.; Carpenter, J. F.; Kita, Y. A.; Crowe, J. H. *Cryobiology* **1990**, *27*, 401.
(2) Yu, Z. W.; Quinn, P. J. *Biosci. Rep.* **1994**, *14*, 259.
(3) Porter, C. J. H.; Trevaskis, N. L.; Charman, W. N. *Nature Rev. Drug Discovery* **2007**, *6*, 231.
(4) Xiang, T.-X.; Anderson, B. D. *Adv. Drug Delivery Rev.* **2006**, *58*, 1357.
(5) Verma, I. M.; Somia, N. *Nature* **1997**, *389*, 239.
(6) Finkelstein, A. *Current topics in membranes and transport*; Academic Press: New York, 1984.
(7) Gordeliy, V. I.; Kiselev, M. A.; Lesieur, P.; Pole, A. V.; Teixeira, J. *Biophys. J.* **1998**, *75*, 2343.
(8) Tristram-Nagle, S.; Moore, T.; Petrache, H. I.; Nagle, J. F. *Biochim. Biophys. Acta, Biomembr.* **1998**, *1369*, 19.
(9) Shashkov, S. N.; Kiselev, M. A.; Tioutiounnikov, S. N.; Kiselev, A. M.; Lesieur, P. *Physica B* **1999**, *271*, 184.
(10) Bemporad, D.; Luttmann, C.; Essex, J. W. *Biochim. Biophys. Acta, Biomembr.* **2005**, *1718*, 1.
(11) Marrink, S. J.; Berendsen, H. J. C. *J. Phys. Chem.* **1994**, *98*, 4155.
(12) Gurtovenko, A. A.; Anwar, J. *J. Phys. Chem. B* **2007**, *111*, 10453.
(13) Leekumjorn, S.; Sum, A. K. *Biochim. Biophys. Acta, Biomembr.* **2006**, *1758*, 1751.
(14) Moldovan, D.; Pinisetty, D.; Devireddy, R. V. *Appl. Phys. Lett.* **2007**, *91*, 204104.
(15) Smondyrev, A. M.; Berkowitz, M. L. *Biophys. J.* **1999**, *76*, 2472.
(16) Sum, A. K.; de Pablo, J. J. *Biophys. J.* **2003**, *85*, 3636.
(17) Notman, R.; Noro, M.; O'Malley, B.; Anwar, J. *J. Am. Chem. Soc.* **2006**, *128*, 13982.
(18) Patra, M.; Salonen, E.; Terama, E.; Vattulainen, I.; Faller, R.; Lee, B. W.; Holopainen, J.; Karttunen, M. *Biophys. J.* **2006**, *90*, 1121.
(19) Pinisetty, D.; Moldovan, D.; Devireddy, R. *Ann. Biomed. Eng.* **2006**, *34*, 1442.
(20) Lindahl, E.; Hess, B.; van der Spoel, D. *J. Mol. Model.* **2001**, *7*, 306.

(21) Berger, O.; Edholm, O.; Jahnig, F. *Biophys. J.* **1997**, *72*, 2002.
(22) Chiu, S. W.; Clark, M.; Balaji, V.; Subramaniam, S.; Scott, H. L.; Jakobsson, E. *Biophys. J.* **1995**, *69*, 1230.
(23) Bordat, P.; Sacristan, J.; Reith, D.; Girard, S.; Glattli, A.; Muller-Plathe, F. *Chem. Phys. Lett.* **2003**, *374*, 201.
(24) Berendsen, H. J. C., Postma, J.P.M.; W. F. van Gunsteren Hermans, J. *Interaction Models for Water in Relation to Protein Hydration*; Reidel: Dordrecht, The Netherlands, 1981.
(25) Hess, B.; Bekker, H.; Berendsen, H. J. C.; Fraaije, J. *J. Comput. Chem.* **1997**, *18*, 1463.
(26) Miyamoto, S.; Kollman, P. A. *J. Comput. Chem.* **1992**, *13*, 952.
(27) Darden, T.; York, D.; Pedersen, L. *J. Chem. Phys.* **1993**, *98*, 10089.
(28) Essmann, U.; Perera, L.; Berkowitz, M. L.; Darden, T.; Lee, H.; Pedersen, L. G. *J. Chem. Phys.* **1995**, *103*, 8577.
(29) den Otter, W. K.; Briels, W. J. *J. Chem. Phys.* **1998**, *109*, 4139.
(30) Den Otter, W. K.; Briels, W. J. *Mol. Phys.* **2000**, *98*, 773.
(31) Ryckaert, J. P.; Ciccotti, G.; Berendsen, H. J. C. *J. Comput. Phys.* **1977**, *23*, 327.
(32) Wohlert, J.; Edholm, O. *Biophys. J.* **2004**, *87*, 2433.
(33) Tieleman, D. P.; Marrink, S. J.; Berendsen, H. J. C. *Biochim. Biophys. Acta, Rev. Biomembr.* **1997**, *1331*, 235.
(34) Gawrisch, K.; Ruston, D.; Zimmerberg, J.; Parsegian, V. A.; Rand, R. P.; Fuller, N. *Biophys. J.* **1992**, *61*, 1213.
(35) Gardiner, C. W. *Handbook of Stochastic Methods: For Physics, Chemistry, and the Natural Sciences*, 3rd ed.; Springer: Berlin, 2004.
(36) Qiao, R.; Roberts, A. P.; Mount, A. S.; Klaine, S. J.; Ke, P. C. *Nano Lett.* **2007**, *7*, 614.
(37) Orsi, M.; Sanderson, W. E.; Essex, J. W. *J. Phys. Chem. B* **2009**, *113*, 12019.